Ground-State Properties of a One–Dimensional System of Hard Rods

F. Mazzanti[1], G. E. Astrakharchik[2], J. Boronat[2], and J. Casulleras[2]

1 *Departament de Física i Enginyeria Nuclear, Comte Urgell 187,*
Universitat Politècnica de Catalunya, E-08036 Barcelona, Spain and
2 *Departament de Física i Enginyeria Nuclear, Campus Nord B4-B5,*
Universitat Politècnica de Catalunya, E-08034 Barcelona, Spain

A quantum Monte Carlo simulation of a system of hard rods in one dimension is presented and discussed. The calculation is exact since the analytical form of the wavefunction is known, and is in excellent agreement with predictions obtained from asymptotic expansions valid at large distances. The analysis of the static structure factor and the pair distribution function indicates that a solid-like and a gas-like phases exist at high and low densities, respectively. The one-body density matrix decays following a power-law at large distances and produces a divergence in the low density momentum distribution at $k = 0$ which can be identified as a quasi-condensate.

Correlated (quasi-)one-dimensional (1D) systems of bosons and fermions have received great attention in the last years due to recent and important experimental progress [1, 2, 3, 4]. The role of quantum fluctuations is enhanced in reduced dimensionalities, producing new and intriguing features different or not present in 3D systems. A well known but striking difference is the nonexistence of a true Bose condensate in 1D homogeneous systems at any temperature [5] (not even at $T = 0$), although it can be realized in trapped systems where the confining potential modifies the atomic density of states [6].

Experimentally, 1D systems can be realized by confining the radial motion of a 3D trapped cloud of cold bosons to zero point oscillations. This is done by acting on the system with two orthogonal standing waves that create an optical lattice containing an array of 1D quantum gases in the axial direction. The ensemble generated in this way allows for a statistical treatment of the relevant quantities being measured. A few years ago, Olshanii [7] showed that in these experiments the scattering length a_{1D} of the resulting systems experience a confined induced resonance according to the expression

$$a_{1D} = \frac{a_\perp^2}{a_{3D}} \left(1 - C \frac{a_{3D}}{a_\perp} \right) , \qquad (1)$$

where a_{3D} is the 3D scattering length of the interatomic potential, $a_\perp = \sqrt{\hbar/m\omega_\perp}$ is the oscillator length of the transverse confinement, and $C = \zeta(1/2)/\sqrt{2} = 1.0326$ with $\zeta(\cdot)$ the Riemann zeta function. In actual experiments, a_{3D} can be tuned to essentially any value in the range $(-\infty, +\infty)$ by exploiting a Feshbach resonance, and thus a_{1D} can be made to vary accordingly, as seen from Eq. (1). In a pseudopotential description, where a_{1D} is directly related to the coupling constant g_{1D} of the contact interaction $U(z) = g_{1D}\delta(z)$ through the relation $g_{1D} = -2\hbar^2/ma_{1D}$ [7], different regimes can be realized when a_{1D} or the density n are changed. These regimes can be classified in terms of the ratio of the interaction energy per particle in a mean-field approximation, $g_{1D}n = -2\hbar^2n/ma_{1D}$, to the characteristic kinetic energy per particle $\hbar^2n^2/2m$. When na_{1D} is large g_{1D}

is small, the effect of correlations is weak and the system enters a mean field regime. As g_{1D} increases, na_{1D} decreases and potential effects are more relevant. In the $na_{1D} \to 0$ limit, g_{1D} goes to infinity and the system becomes a Tonks-Girardeau gas of impenetrable bosons [8]. In this regime, correlations are so strong that the ground-state wave function acquires a fermionic behavior and it vanishes when two or more particles meet [8, 9]. More recently, a new state called super-Tonks-Girardeau, corresponding to $g_{1D} \to -\infty$, has been identified and shown to exhibit even stronger correlation effects [10]. In this regime the system behaves as a gas of hard rods of length $a = a_{1D}$ for particle densities $na_{1D} \leq 0.1$. At higher densities, the interatomic potential of a system of hard rods is no longer *weak* for a pseudopotential picture to be realistic. Nevertheless, at high densities the hard rods model can be used to understand static and dynamic properties of strongly correlated 1D systems with higly repulsive interactions at short distances, like He or other gases adsorbed in Carbon nanotubes [11, 12].

Hard rods are the 1D counterpart of hard spheres in 3D [13, 14]. The interatomic rod potential reads $V_{HR}(z) = +\infty$ for $|z| < a$ and 0 otherwise. The associated N–particle Hamiltonian becomes

$$H = -\frac{\hbar^2}{2m} \sum_{j=1}^{N} \frac{\partial^2}{\partial z_j^2} + \sum_{i<j} V_{HR}(z_{ij}) . \qquad (2)$$

whith the *exact* ground-state wavefunction [15]

$$\Psi_0(z_1, z_2, ..., z_N) = \frac{1}{\sqrt{N!}} \left| \det \left(\frac{1}{\sqrt{L'}} \exp(ip'_k x_k) \right) \right| . \quad (3)$$

In this expression, $L' = L - aN$ is the *unexcluded* volume, $\{p'_k = 2\pi n_k/L'\}$ are a set of quantum numbers with $n_k \in [-N, +N]$, and $x_k = z_k - (k-1)a$ are the so–called rod coordinates corresponding to a given ordering of the true particle coordinates $z_1 < z_2 - a < z_3 - 2a < \cdots < z_N - a(N-1)$. As in the 3D case of hard spheres, the scattering length of the hard rod potential equals the size of the rod, $a_{1D} = a$.

Despite the fact that the analytical form of the ground-state wavefunction is known, limited progress has been achieved in the description of this system [16, 17]. In this work, we analyze and discuss the static properties of a gas of hard rods of length a at $T = 0$ as a function of the density by means of Monte Carlo simulations. We sample the wavefunction (3) using the Metropolis algorithm and impose periodic boundary conditions for a number of particles in the range $N \leq 300$. Notice that since this wavefunction is the exact solution to the N–body problem corresponding to the Hamiltonian in Eq. (2), the results of the simulations are statistically exact. As a check to the calculation we reproduce numerically with zero variance the equation of state of the system, whose analytical expression reads

$$\frac{E_{HR}}{N} = \frac{\pi^2 \hbar^2 n^2}{6m} \frac{1}{(1 - na)^2} \ . \qquad (4)$$

We first analyze the static structure factor $S(k) = \langle \Psi_0 \mid \rho_k^\dagger \rho_k \mid \Psi_0 \rangle / N$, with $\rho_k = \sum_{j=1}^N e^{ikz_j}$ the density fluctuation operator. Even though the ground-state wave function is known, no simple analytical expression can be easily derived for $S(k)$, although three notorious properties can be inferred. On one hand, the system is a realization of a Luttinger liquid with low k excitations dominated by phonons [18], and therefore $S(k \to 0) = \hbar|k|/2mc$. The speed of sound c can be obtained from the equation of state (4) and leads to

$$S(k \to 0) \approx \frac{(1 - an)^2}{2\pi n} |k| \ . \qquad (5)$$

On the other hand and for a given particle ordering, the density fluctuation operator becomes $\rho_k = \sum_{j=1}^N e^{ikx_j}$ when k is a multiple of $2\pi/a$. In this case, the a factors in the change to rod coordinates $\{z_k\} \to \{x_k\}$ have no influence in $S(k)$, which equals the corresponding value of the static structure factor of the 1D free Fermi gas (FFG) at the rod density $n' = n/(1 - an)$

$$S_{FFG}(k) = \begin{cases} \frac{1-an}{2\pi n} |k| & \text{for } |k| \leq \frac{2\pi n}{1-an} \\ 1 & \text{otherwise} \ . \end{cases} \qquad (6)$$

Introducing explicitly the change to rod coordinates, $S(k)$ can be written in the exact form

$$S(k) = 1 + 2(N-1)! \sum_{i=1}^{N-1} \sum_{j=1}^{N-i} \int_{\Omega_N} dx^N \cos\left[k(x_{i+j,i} + ja)\right] \Psi_0^2 \qquad (7)$$

where $x_{i,j} = x_i - x_j$, Ω_N denotes the integration region $0 \leq x_1 < x_2 < \cdots < x_N \leq L'$ and Ψ_0 is the Slater determinant of Eq. (3). Due to strong correlations the most probable configurations are those where all particles are equally spaced at a distance $\Delta x = L'/N$. The contribution to $S(k)$ becomes maximal when all the cosine terms in Eq. (7) equal 1 for these configurations, which
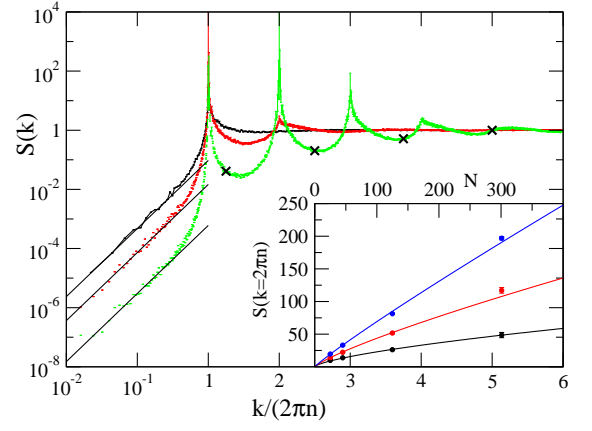

FIG. 1: (Color online) $S(k)$ at particle densities $na = 0.4, 0.6$ and 0.8 (upper, middle and lower cures at low k). Notice the logarithmic scale up to $k/2\pi n = 1$. Solid line: phononic behavior of Eq. (5). The crosses correspond to the exact values from Eq. (6), for $na = 0.8$ at $k_i = 2\pi i/a, i = 1, 2, 3, 4$. Inset: height of the first peak as a function of the total number of particles (symbols) for densities $na = 0.6, 0.7$ and 0.8 (lower, middle and upper curves, respectively), best fit with the law given by Eq. 9 and $m = 1$ (lines).

happens at the discrete values $k_j = 2\pi nj$. In summary, one expects an $S(k)$ growing linearly at low k, presenting an infinite number of equally spaced maxima, and approaching the asymptotic value of 1 when $k \to \infty$.

Results for $S(k)$ at three different densities are shown in Fig. 1. A logarithmic scale up to $k/2\pi n = 1$ has been used to emphasize the $k \to 0$ linear behavior of $S(k)$ given in Eq. (5). The upper, middle and lower curves in that region correspond to $na = 0.4, 0.6$ and 0.8, respectively. At lower densities $na \leq 0.1$, $S(k)$ is much smoother and approaches the hard point limiting case of Eq. (6). The crosses in the plot correspond to the exact values obtained from this equation at $k_i = 2\pi i/a$. As it can be seen from the figure, the peaks at $k_j = 2\pi nj$ are enhanced at higher densities while at intermediate values the strength is depressed. Our simulations indicate that the height of the peaks increases with the particle number at large densities. This dependence can be understood by looking at the asymptotic expansion of the pair distribution function, the Fourier transform of $S(k)$, which admits, for a Luttinger liquid and according to Haldane [18], the following asymptotic expansion valid when $|z| \gg n^{-1}$

$$g(z) = 1 - \frac{\eta}{(2\pi n z)^2} + \sum_{m=1}^\infty A_m \frac{\cos(2\pi n m z)}{(n|z|)^{m^2 \eta}} \ , \qquad (8)$$

where $\eta = 2K$ and $K = \pi \hbar n / mc$ is the Luttinger parameter, while the coefficients A_m depend both on the density and the system under study. Notice that the z^{-2} term coming from density-density fluctuations determines the low k behavior of $S(k)$ reported in Eq. (7).
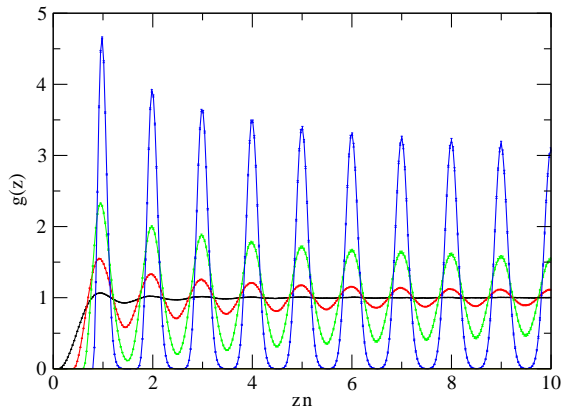
FIG. 2: (Color online) Two-body radial distribution function at different densities. From top to bottom: $na = 0.8, 0.6, 0.4$ and 0.1, respectively.

Furthermore, $\eta = 2(1 - na)^2$ for a system of hard rods while $\eta = 2$ for the 1D free Fermi gas. According to this expression, the height of the m-th peak follows a power-law of the form $|z|^{1-m^2\eta}$. The inset in Fig. 1 shows the height of the first peak as a function of the number of particles in the simulation compared with the corresponding curves

$$S(k = 2m\pi n) = A_m N^{1-2m^2(1-na)^2}, \tag{9}$$

with $m = 1$ corresponding to the first peak. A fit to the Monte Carlo data shows that these curves are compatible with the choice $A_1 = 1$ at high densities. Furthermore, the law (9) predicts that only a finite number of macroscopic peaks located at $k_m = 2\pi nm$ and satisfying the inequality $1 - 2m^2(1-na)^2 > 0$ exist. In the case $na = 0.8$ this implies that $m < 3.5$, and we find only three peaks whose height grows with the number of particles. The linear behavior $S(k) \propto N$ at the peak, characteristic of 3D crystals, is recovered asymptotically as $na \to 1$. All these facts suggest that a packing order, resulting from the combined effect of particle correlations and the reduced dimensionality, shows up at high densities, thus manifesting the existence of a *quasi–solid* phase. At low density these effects, although present, are much less evident, as the peaks are washed out at $na \ll 1$ and $S(k)$ approaches the simple structure corresponding to a 1D free Fermi gas with the density $n' = n/(1-an)$ reported in Eq. (6). In this sense, the system of hard rods clearly presents different regimes and behaves as a *quasi–solid* at high densities.

The pair distribution function $g(z)$ is depicted in Fig. 2 for several densities. Being related to $S(k)$ by a Fourier transformation, it reproduces the same packing structure and particularly presents a series of peaks located at multiples of $1/n$, coming from the $m = 1$ term in Eq. (8). As in the case of $S(k)$, the strength of the peaks increase with the density, while in all situations $g(z) = 0$ inside

the core of the potential $|z| < a$. At the lowest densities, $g(z)$ approaches the hard point limit corresponding to the 1D free Fermi gas

$$g_{HP}(z) = 1 - \frac{\sin^2(\pi nz)}{N^2 \sin^2(\pi nz/N)} \tag{10}$$

with n' replaced by n since the distinction between them is not important at low densities. This function presents a periodic structure with $N/2$ equally spaced peaks in the range $[0, L/2]$. In the thermodynamic limit, $g_{HP}(z)$ admits an expression of the form (8) with $\eta = 2$ and $A_m = (2\pi^2)^{-1}\delta_{m,1}$, with a single frequency contributing to the oscillations. In the case of hard rods, the peaks remain at the same location and are enhanced as the density is increased, which indicates that the number of peaks extends to infinity in the thermodynamic limit.

The next quantity analyzed is the off-diagonal one–body density matrix. From translational invariance arguments and the normalization of the wave function it follows that $n_1(0) = n$. In systems of higher dimensionality, the presence of a Bose condensate with density n_0 induces non–diagonal long range order that is manifested in a finite asymptotic value $n_1(|z| \to \infty) = n_0 > 0$. This is not the case in homogeneous 1D systems, where a true BEC is suppressed and thus $n_1(|z| \to \infty) \to 0$. Figure (3) shows the one–body density matrix in logarithmic scale and for the three densities $na = 0.2, 0.4$ and 0.6. Clearly, $n_1(z)$ shows an oscillating structure that expresses the presence of an excluded length corresponding to the rod size.

Uniform Bose Luttinger liquids admit an asymptotic expansion valid at large distances of the form [18]

$$\frac{n_1(z)}{n} = \frac{1}{(n|z|)^{1/\eta}} \sum_{m=0}^{\infty} B_m \frac{\cos(2\pi n\,m\,z)}{(n|z|)^{m^2\eta}} , \tag{11}$$
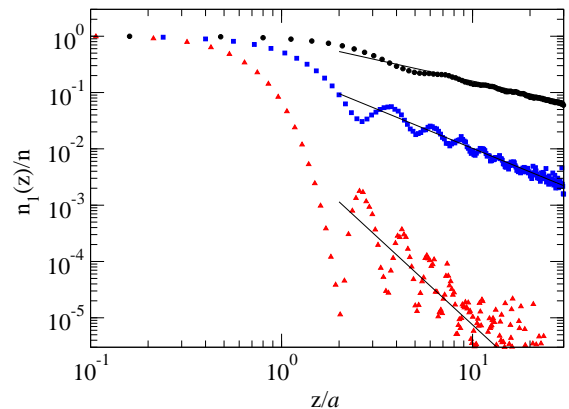

FIG. 3: (Color online) One–body density matrix at the densities $na = 0.2, 0.4$ and 0.6 (upper, middle and lower curves, respectively). The solid lines represent the asymptotic behavior at long distances.

and thus the long range behavior of $n_1(z)$ depends on the value of the Luttinger parameter η. For hard rods this means that $n_1(|z| \gg 1)$ decays following a $|z|^{-1/2(1-an)^2}$ power law. A fit to the tail of the data of this analytical form is also shown in Fig. (3) for each density.

The momentum distribution $n(k)$, which describes the occupation of each single–particle state of momentum k, is the Fourier transform of the one–body density matrix. Fig. 4 displays $n(k)$ for three different densities. The large z power law decay of the one–body density matrix makes the low k behavior of $n(k)$ depend on η. For hard rods $\eta = 2(1 - na)^2$ and that dependence defines a critical density $n_c a = 1 - 1/\sqrt{2} \approx 0.29$ separating two different regimes. At lower densities the momentum distribution presents an infrared divergence of the form $k^{1-1/2(1-na)^2}$ and a discontinuity in the first derivative at $k = 2\pi n$, as can be checked by direct inspection of the Fourier transform of the $m = 0$ and $m = 1$ terms in Eq. (11). Both features disappear at higher densities, although a change in the slope of $n(k)$ is still noticeable at intermediate values of na. The inset in Fig. 4 shows the product $k^{1-1/2(1-na)^2} n(k)$ for two densities. The divergence of $n(k = 0)$ can be interpreted as the manifestation of a Bose–Einstein quasi–condensate, while the kink at $k = 2\pi n$ is a reminiscence of the underlaying fermionic nature of the wave function, as for 1D Fermions $k_F = \pi n$.

We end up this discussion by noticing that the arguments leading to the exact values of $S(k)$ at $k_j = 2\pi j/a$ can be extended to predict the behavior of the $T = 0$ dynamic structure function $S(k, \omega)$ at these same momenta, which equals that of the 1D free Fermi gas at the equivalent density $n' = n/(1 - an)$

$$ S\left(k_j = \frac{2\pi j}{a}, \omega\right) = \begin{cases} \frac{1-an}{2\pi n}\left(\frac{m}{k_j}\right) & ; \ \omega \in (\omega_0, \omega_1) \\ 0 & \text{otherwise} \end{cases} $$

(12)

with $\omega_0 = |\, k_j^2/2m - \pi k_j n/(1 - an)\,|$ and $\omega_1 = k_j^2/2m + \pi k_j n/(1 - an)$. In this way, $S(k = k_j, \omega)$ becomes a constant independent of ω in the range (ω_0, ω_1), and leads to the finite values of $S(k)$ reported in Eq. (6) once integrated. At different momenta $k \neq k_j$, $S(k, \omega)$ is expected to present at least one peak that increases when k approaches the values $k_i = 2\pi n i$ where $S(k)$ diverges in the thermodynamic limit.

In summary, we have carried out a complete study of the most relevant one- and two- body correlation functions for a system of hard-rods at $T = 0$. We find two distinct regimes where the system behaves as a gas (low density) and as a quasi-solid (large density), without any signature of a phase transition in the energy. The quasi-solid regime is characterized by the presence of macroscopic peaks in the static structure factor. The one–body density matrix at large distances decays following a power law that leads to a divergence of the low density momentum distribution at $k = 0$. This divergence can be understood as the manifestation of a Bose–Einstein quasi-condensate. Finally, exact values for the static structure factor and dynamic structure function at the momenta $k_j = 2\pi j/a$ have also been reported. Our results allow for a much better understanding of the fundamental hard rod model. We hope our work can stimulate further experimental work both in dilute vapors and in condensed phases in 1D systems.
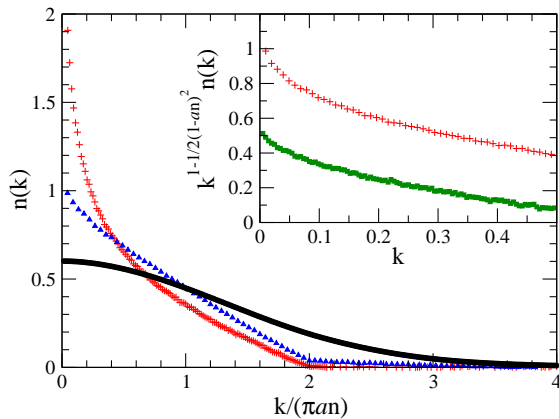
FIG. 4: (Color online) Momentum distribution $n(k)$ of the hard rods system at the densities $na = 0.2, 0.4$ and 0.6 (upper, middle and lower curves). The inset shows the product $k^{1-1/\eta} n(k)$ at $na = 0.1$ (squares) and $na = 0.2$ (stars).

[1] B. Paredes *et al.*, Nature **429**, 277 (2004).
[2] I. Bloch, Nature Phys. **1**, 23 (2005).
[3] H. Moritz *et al*, Phys. Rev. Lett. **91**, 250402 (2003).
[4] S. Richard *et al.*, Phys. Rev. Lett. **91**, 010405 (2003).
[5] P. C. Hohenberg, Phys. Rev. **158**, 383 (1967).
[6] A. Görlitz, *et al.*, Phys. Rev. Lett. **87**, 130402 (2001).
[7] M. Olshanii, Phys. Rev. Lett. **81**, 938 (1998).
[8] M. Girardeau, J.Math.Phys. **1**, 516 (1960).
[9] E. H. Lieb and W. Liniger, Phys. Rev. **130**, 1605 (1963).
[10] G. E. Astrakharchik *et al*, Phys. Rev. Lett. **95**, 190407 (2005).
[11] J. V. Pearce *et al*, Phys. Rev. Lett. **95**, 185302 (2005).
[12] M. Mercedes *et al.*, Rev. Mod. Phys. **73**, 857 (2001).
[13] S. Giorgini, J. Boronat, and J. Casulleras, Phys. Rev. A**60**, 5129 (1999).
[14] F. Mazzanti, A. Polls, and A. Fabrocini, Phys. Rev. A**67**, 063615 (2003)

[15] T. Nagamiya, Proc. Phys. Math. Soc. Jpn. **22**, 705 (1940).

[16] R. J. Rubin, J. Chem. Phys. **23**, 1183 (1955).

[17] E. Krotscheck, M. D. Miller and J. Wojdylo, Phys. Rev. B**60**, 13028 (1999).

[18] F. D. M. Haldane, Phys. Rev. Lett. **47**, 1840 (1981).